Microchemical Journal 160 (2021) 105690

Contents lists available at ScienceDirect

Microchemical Journal

journal homepage: www.elsevier.com/locate/microc

Microplastic abundance quantification via a computer-vision-based chemometrics-assisted approach

Crislaine Bertoldi, Larissa Z. Lara, Adriano A. Gomes, Andreia N. Fernandes *

Instituto de Química, Universidade Federal do Rio Grande do Sul (UFRGS), Av. Bento Gonçalves, 9500, Porto Alegre-RS 91501-970, Brazil

ARTICLE INFO

Keywords:
Image processing
Colour histogram
Multivariate calibration
Microplastic contamination

ABSTRACT

Microplastic (MP) contamination is a topic of growing global concern; these particles are ubiquitous in environmental ecosystems and have been found in aquatic, terrestrial, and atmospheric mediums. However, the protocols to quantify MPs in environmental samples have limitations and may lead to overestimation and/or underestimation of the plastic debris. Therefore, the aim of this research was to develop a simple procedure to determine the abundance of MPs using digital image processing and chemometric treatment. The proposed method combined computer-vision-based and multivariate calibration by partial least squares coupled with interval selection (*i*PLS and successive algorithm projection - *i*SPA). The abundance ranges of the yellow, blue, black, colourless, green, and red MPs were 1–212, 7–134, 0–50, 6–290, 0–113, and 20–392, respectively. When the models were applied to an independent set of samples, the following RMSEP values were found: 9.8 (yellow), 6.4 (blue), 3.5 (black), 8.1 (colourless), 7.5 (green), and 19.3 (red). The results showed that image processing has the potential to quantify MPs with respect their colour. This method could help to reduce time-consuming and to avoid subjectivity in future analyses.

1. Introduction

Global plastic production has increased annually, with 359 million tons of plastic produced in 2018 [1]. The major problem with plastics is their inadequate disposal, resulting in pollution and their accumulate in the environment. Once in an environmental system, plastics may be subjected to different types of degradation and fragmentation, such as photooxidation and thermal oxidation by sun radiation, as well as hydrolysis and biological and mechanical stressors [2–4]. These processes generate smaller pieces of plastics called microplastics (MPs), which are particles defined as having a diameter in the range of 1 μm to 5 mm [5].

The MPs are divided into primary and secondary sources according to their origin. Primary source MPs are produced intentionally in a specific size [6]. For instance, small fragments and pellets are used in personal care products (shower gel, facial cleanser, hand sanitiser, and soap) [7], paint [8], and agriculture (encapsulation of fungicides and/or insecticides in film coatings) [9]. Secondary MPs are generated by fragmentation and/or degradation of larger plastics, such as single-use packaging [10] and fibres from washing clothes [11]. These MPs can enter aquatic bodies through direct disposal of waste as a result of poor waste management systems, surface runoff, sewage sludge, and wind transportation of MPs in the atmosphere [6,12,13].

Once in the aquatic environment, these MPs interact with the aquatic biota, and their ingestion has become frequently reported. Due to their similar size as plankton, MPs can easily be mistaken by natural prey and can cause severe injuries to organisms, such as starvation, bowel perforations, and endocrine disruption [14,15]. Their morphological properties and hydrophobicity have made these particles potential vectors of organic compounds and heavy metals; thus, their intake might result in bioaccumulation of these contaminants [16,17]. In addition, MPs with diameters smaller than 20 μm can also enter the circulatory system of human beings and potentially harm the human body [18].

The identification and quantification of MPs is generally performed by physical and chemical characterisation. Physical characterisation, which is done by visual inspection (naked eye) or with microscopes, is one of the most used methods of identification and quantification of plastic particles [2] since it is widely available in labs, it is simple to operate, and it is cheap. However, this method may generate wide variations and it is highly time consuming. It is reported in the literature that the detection of MPs by visual inspection can vary considerably depending on the individual observer, observer experience, and fatigue (i.e., reduced vigilance). In addition, overestimation (e.g., count of

* Corresponding author.
E-mail address: andreia.fernandes@ufrgs.br (A.N. Fernandes).

https://doi.org/10.1016/j.microc.2020.105690
Received 22 September 2020; Received in revised form 28 October 2020; Accepted 28 October 2020
Available online 4 November 2020

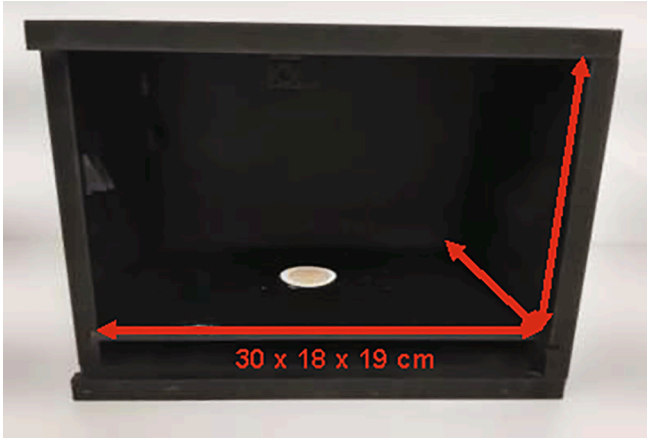

Fig. 1. Acquisition system used to take digital images of each filter sample.

biological material as microplastics) and/or underestimation (caused by white fragments) may lead to a misclassification of the number of coloured fragments [19,20]. In view of the limitations, the development of new methods to detect and quantify MPs is highly urgent. Thus, chemometric treatment combined with image processing is a powerful tool that can be used to solve the problem with the visual inspection of MPs in environmental samples. In the literature, there are approaches that already use chemometric tools with hyperspectral imaging employing infra-red spectrometry and Raman technique, even though these methods are expensive and can generate a large amount of data for treatment [21,22]. In this sense, the main objective of the present study was to develop a simple procedure to determine MPs by image processing combined with chemometric treatment.

2. Experimental

2.1. Samples

In total, 32 surface water samples were collected in Guaíba Lake, Porto Alegre, Brazil. For sampling, a net with a mesh size of 60 μm was used. The net had a 0.30 × 0.70 m opening, with a total area of 0.071 m^2, containing a 150 mL collecting cylinder at the conical end. The net was towed horizontally on the surface for 10 min at a speed of 3 km h^{-1}. Then, it was retrieved, and the water collected was transferred to a clean glass vial flask. All samples were collected in the same manner. After sampling, samples were stored at 0 °C and processed as soon as possible.

The method for sample processing was followed according to a modified procedure by the National Oceanic and Atmospheric Administration (NOAA) [23]. To separate MPs, the water was filtered with a 63 μm stainless-steel sieve, and then the sieve was washed with ultrapure water (Milli-Q) to remove the solid residue. The sample was submitted to wet peroxide oxidation (WPO) to reduce the amount of organic matter. For WPO, 20 mL of a 0.05 M Fe(II) solution in acidic medium (0.1 M H_2SO_4) and 20 mL of 35% H_2O_2 were added to the beaker containing the solid material. Subsequently, the mixture was placed on a 60 °C hotplate and stirred for 1 h. After the WPO procedure, the sample was covered with aluminium foil and left at room temperature for 24 h. Consequently, the sample was filtered with a cellulose acetate filter (0.45 μm), washed with sodium iodine (1.6 g cm^{-3}), and settled down for 24 h in a separator flask. After the density separation process, it was expected that the plastic material would float and the inorganic material would be deposited as sediment, which would allow us to drain the rejected material. Then, the remaining sample was filtered with a glass fibre filter (0.45 μm pore size), and the funnel was washed many times to ensure that all the particles were transferred to the membrane. Lastly, the membrane was dried at room temperature in petri dishes until characterisation. During sample processing, all materials were carefully washed with ultrapure water (Milli-Q) to avoid MP contamination from the laboratory.

Table 1
Minimum, maximum, and average values of microplastics counted in the samples through visual inspection.

Color	Minimum	Maximum	Average	Standard deviation
Yellow	1	212	48	38
Blue	7	134	43	23
Black	0	50	6	6
Colorless	6	290	85	64
Green	0	113	26	22
Red	20	329	73	38

2.2. Microplastic quantitation by visual inspection

Visual inspection was performed using an Olympus BX41 stereomicroscope (4× and 10× magnification) to count and categorise the MPs. The particles were counted and categorised according to their colours and divided into the following six classes: colourless, red, blue, green, black, and yellow.

2.3. Digital image acquisition

Digital image acquisition was carried out using the system shown in Fig. 1, which is a wood box with dimensions of 30 × 18 × 19 cm. This system was used to equalise and isolate the sample from the external light. The images were taken with a 12 Mp camera (each image had 4032 × 3016 pixels), which was positioned 10 cm from the sample at 90° relative to the filter containing the MPs. All images were taken following the same procedure. The lighting of the camera itself was kept constant during the acquisition of all images, which were stored in the JPEG extension with both horizontal and vertical resolution of 96 dpi and 24 bits. At the time of registering the images, the box was closed, and the webcam was handled via a laptop.

2.4. Chemometrics procedures

Each image was processed with an *ImageGUI* MATLAB routine in order to generate a colour histogram for grey scale, red, green, blue, hue, saturation, and value. Each colour channel comprised 256 colour levels and the full data matrix was 32 × 1792 in size. The data set was partitioned using sample partition (calibration, 20 samples; external prediction set, 12 samples) using X and Y joint distance as described elsewhere [24]. Multivariate calibration models were built via partial least squares (PLS) [25], and variable selection was performed using intervals (i) and the interval successive projection algorithm (*i*SPA), both coupled to PLS [26]. The smallest error by full cross validation (leave one out) was taken into account to determine the reliable number of latent variable (LV) for each model. All calculations were carried out in MATLAB environmental 2010a using the MCV1 toolbox (available at https://www.iquir-conicet.gov.ar/esp/pers2.php?campo1=82&area=12) [27] and a homemade MATLAB toolbox (available by request at araujo.gomes@ufrgs.br).

3. Results and discussion

3.1. Visual inspection

MP counts are useful for monitoring the presence of polymeric debris

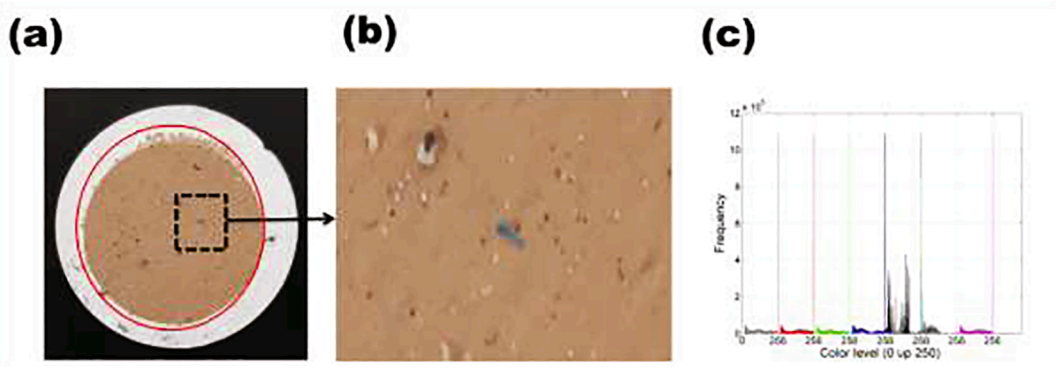

Fig. 2. Data set: in (a) digital image; (b) it zooms showing details of processed images; and (c) full histogram from all samples. Black and magenta colours correspond to hue, saturation, and value, respectively. Other colour models are properly indexed.

Table 2
Statistical summary for calibration, cross validation, and prediction. [a/b]Number of intervals selected/number of intervals in which the histogram was partitioned.

Model	*i*SPAPLS	PLS	*i*SPAPLS	*i*PLS	*i*PLS	*i*SPAPLS
Color	Yellow	Blue	Black	Colorless	Green	Red
LV	3	2	1	2	3	2
Intervals[a/b]	12/15	1/1	1/10	1/10	1/20	1/10
RMSEC	3.4	7.0	5.0	13.7	5.7	28.7
RMSECV	5.3	8.6	5.7	16.5	6.4	35.5
R^2-cv	0.98	0.92	0.69	0.78	0.87	0.91
RMSEP	9.8	6.4	3.5	8.1	7.5	19.3
R^2-pred	0.90	0.83	0.87	0.56	0.69	0.49

[a/b] Number of intervals selected/number of intervals in which the histogram was partitioned.

in the aquatic environment. However, the main tool used for this objective was visual inspection, which showed many sources of error during the counts. The visual count is highly influenced by the observer experience as well as the characteristics of the sample since it has been observed that organic materials, such as twigs and tree leaves, can be identified as MPs [19]. These facts might lead to an underestimation or overestimation of the total number of MPs. Among the studied samples, the colourless and red MPs were the predominant colours. Table 1 shows the minimum, maximum, and average of microplastics number counted between the two counts. The highest deviation was obtained for the colourless samples, followed by the yellow and red samples. This is probably because these MPs can be mistaken with organic or cellulosic materials.

These findings agree with a study reported by Lavers et al., who found high variation among the different counts of MPs, which was around 60% to 100% variability. This study suggested that several factors may impact the MP counts, such as observer experience, visibility of the MP in the samples, and mistaking biological and organic material with plastic debris. Other research performed by Song et al. [28] has shown that the number of MPs can have high variation upon visual inspection compared to Fourier-transform infrared spectroscopy (FT-IR) analysis, with error rates up to 70%. Therefore, these results show the extreme variance that may be occur during visual detection.

3.2. Calibration and validations models

In Fig. 2a, a typical digital image processed in this work is depicted; organic matter and soil remnants generate a coloured background in brown tones. Larger pieces of plastics are easily seen, as in the case of the blue fragment shown in detail in Fig. 2b. The red circle corresponds to the definition of the region of interest (ROI) for the maintenance of colour histograms shown in Fig. 2c. Practically all colour levels exhibit non-zero frequency, showing sample complexity.

The calibration models based on PLS were built, and variable selection was performed by means of the *i*PLS and *i*SPA-PLS approaches. Interval widths of 5, 10, 15, and 20 were evaluated against the root mean square error of cross validation (RMSECV), and the minimum one for each colour of plastic was selected.

A statistical summary of fitness, validation, and prediction are shown in Table 2, and it can be seen that the digital images carry the appropriate information needed to model the amount of MPs. Considering all cases, the largest number of latent variables chosen was 3, suggesting parsimonious models. The calibration (RMSEC) and cross-validation (RMSECV) error values agreed with each other, indicating that the models do not exhibit overfitting. Considering the complexity and subjectivity of the visual counting method, the statistical summary for prediction also displays acceptable values.

For the blue colour, the best model was the full PLS. For all other cases, subsets of intervals showed better results (see Fig. 3). And except for yellow, all others models based on variable selection exhibited a single interval as the best solution. For the yellow colour, the selected ranges included the grey scale and all the colours of the RGB system, in addition to all saturation levels. Interestingly, the model for black-coloured MPs showed better results for the model employing the hue colour levels. The model for colourless MPs was better fitted using only saturation and value information. The model for green MPs selected a narrow range, including shades of black and red, and the last model (model for red colour) showed better results when only saturation information was included.

Fig. 4 depicts the predicted versus reference values for all cases. As can be seen, although the reference method has a high level of subjectivity, reasonable correlations were obtained between nominal values and predicted by the PLS models. Predicted values in the cross validation and independent test set fit across the bisector. The PLS validation procedure was carried out by means of leave-one-out cross validation in order to find the appropriate number of variable laments (VL), and the optimum was chosen by the Haaland – Thomas approach. This information is shown in Table 2. The optimal number of latent variables was used to predict an independent test set. In addition, Fig. 5 represents the elliptical joint confidence regions (EJCR) for slope and intercept from the fitted line to predict versus reference values the elliptical region was designed for 95% statistical confidence.

As can be seen, models for the colours blue, yellow, and red do not exhibit significant bias. On the other hand, green, black, and colourless

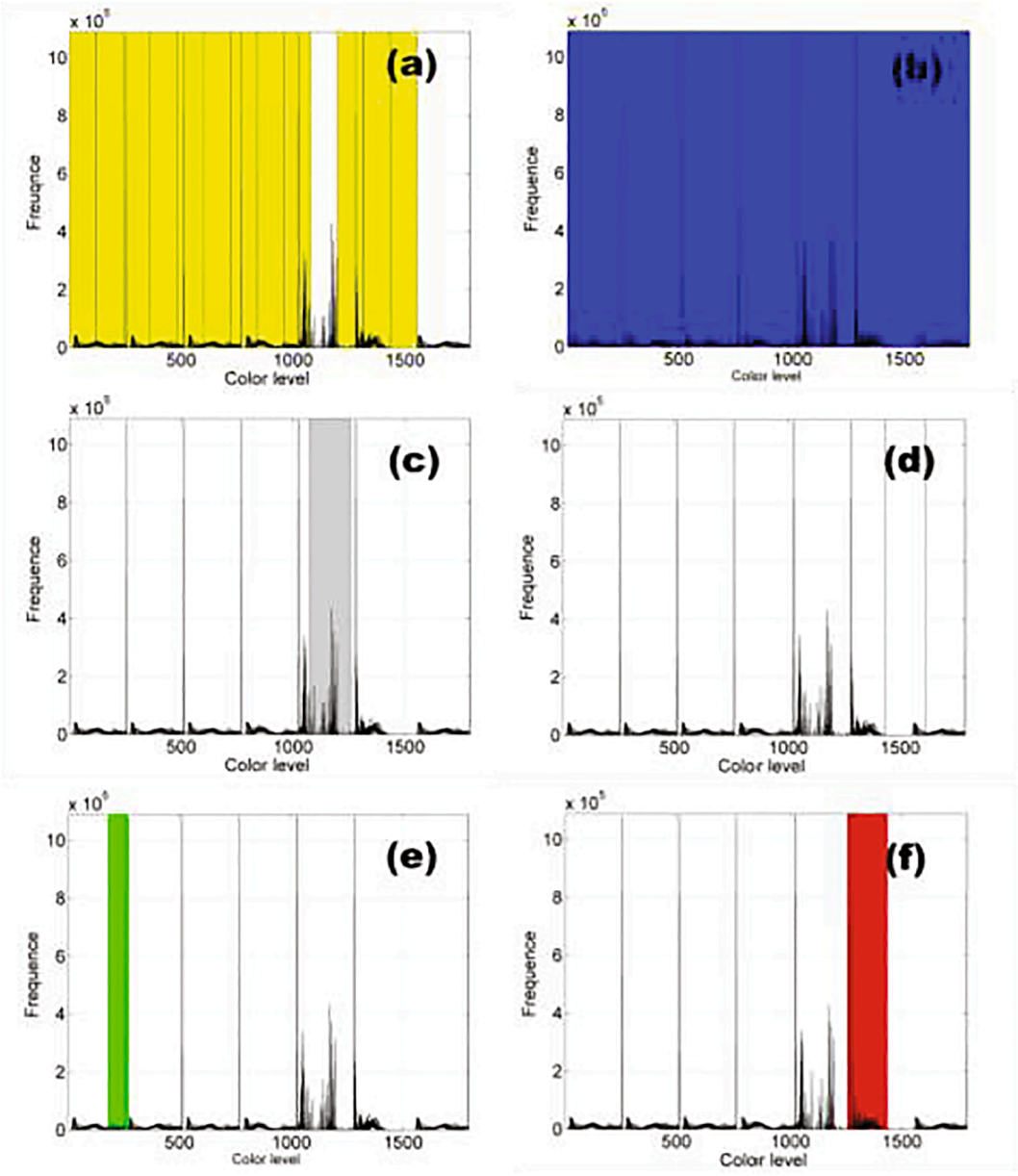

Fig. 3. Variables included in each model. (a) Yellow, (b) blue, (c) black, (d) colourless, (e) green, and (f) red.

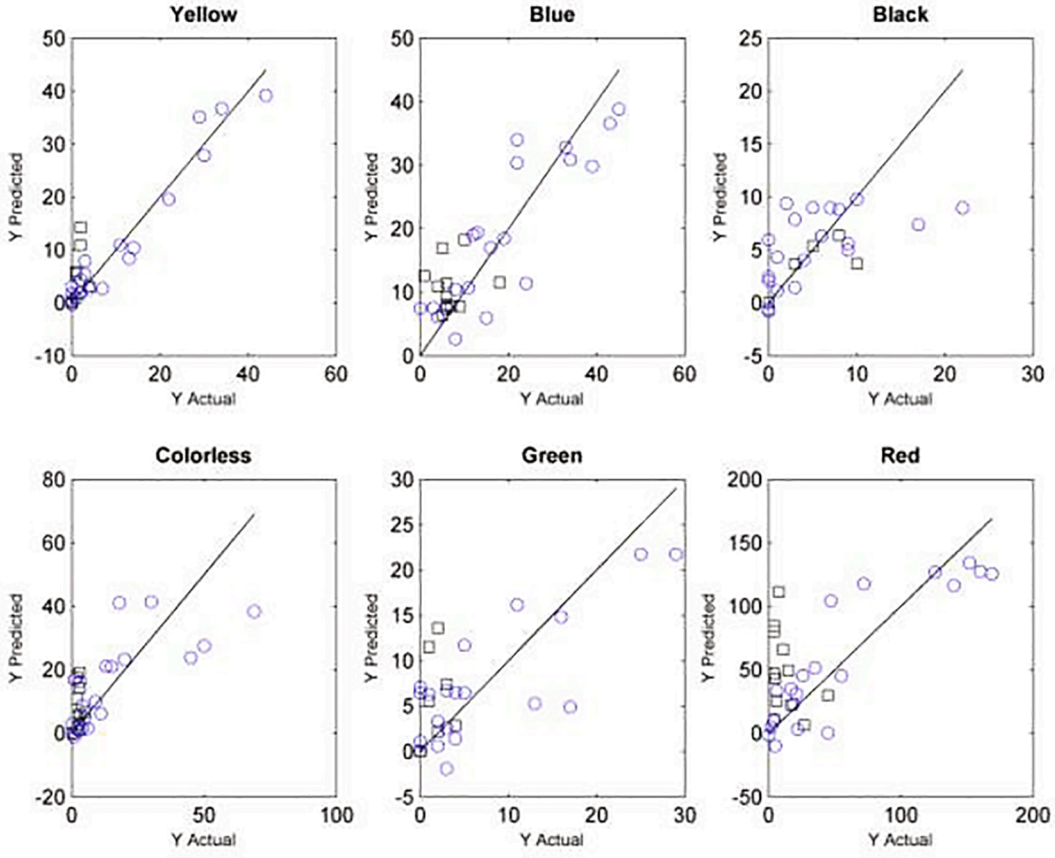

Fig. 4. Predicted versus reference for all cases. The blue ball and black square are values computed for cross validation and the external test set, respectively.

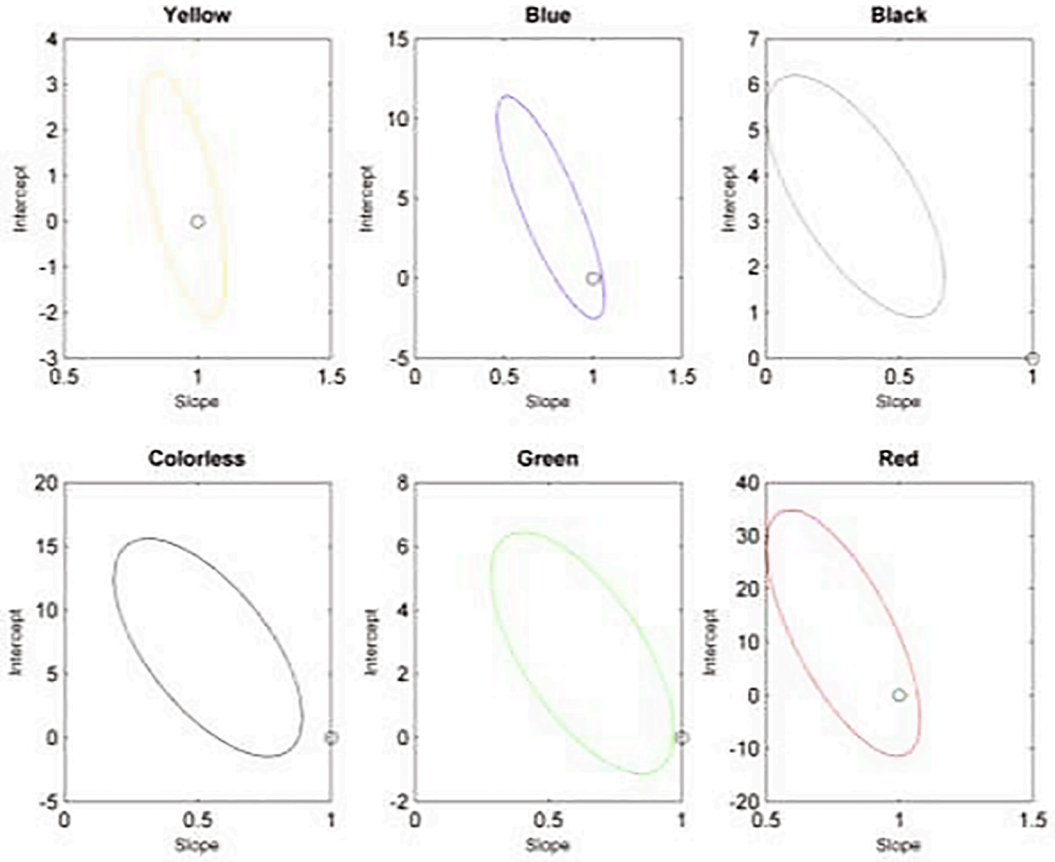

Fig. 5. Elliptical joint confidence regions for cross validation.

models exhibited a slight proportional bias. In any case, the results obtained indicate a permissive approach as a viable alternative to visual inspection and manual counting. The obtained difference between the visual and chemometric methods is probably caused by the interference of organic and biological material in MP identification, but also by observer fatigue. Moreover, the overestimation of the amount of MPs could occur since this approach characterises MP content by colour, and natural fibres may be coloured and may be mistaken as MPs, demonstrating a limitation of the method that should be further improved upon.

4. Conclusion

This study proposed a computer-vision-based chemometrics-assisted approach devoted to determining the abundance of MPs using digital image processing was reported. Based on these findings, it is possible to point out that the described approach has great potential to replace visual inspection. The approach presented here is fast, inexpensive, and accessible, even to governments in developing countries. Last but not least, it eliminates the effect of human subjectivity in future analyses.

CRediT authorship contribution statement

Crislaine Bertoldi: Conceptualization, Software, Formal analysis, Investigation, Methodology, Writing - original draft. **Larissa Z. Lara:** Conceptualization, Investigation, Writing - original draft. **Adriano A. Gomes:** Conceptualization, Software, Formal analysis, Writing - review & editing. **Andreia N. Fernandes:** Investigation, Resources, Writing - review & editing, Supervision, Project administration, Funding acquisition.

Declaration of Competing Interest

The authors declare that they have no known competing financial interests or personal relationships that could have appeared to influence the work reported in this paper.

Acknowledgements

The authors thank the Coordination for the Improvement of Higher Education Personnel (CAPES, Finance Code 001) and the National Institute for Advanced Analytical Science and Technology (INCTAA, CNPqproc. 465768/2014-8) for financial support.

Appendix A. Supplementary data

Supplementary data to this article can be found online at https://doi.org/10.1016/j.microc.2020.105690.

References

[1] PlasticsEurope, Plastics – the Facts 2019, 2019.
[2] J.C. Prata, J.P. da Costa, A.C. Duarte, T. Rocha-Santos, Methods for sampling and detection of microplastics in water and sediment: A critical review, TrAC, Trends Anal. Chem. 110 (2019) 150–159, https://doi.org/10.1016/j.trac.2018.10.029.
[3] A.L. Andrady, Microplastics in the marine environment, Mar. Pollut. Bull. 62 (8) (2011) 1596–1605, https://doi.org/10.1016/j.marpolbul.2011.05.030.
[4] C.B. Crawford, B. Quinn, Microplastic Pollut. (2016), https://doi.org/10.1016/B978-0-12-809406-8.00006-2.
[5] R.C. Thompson, Y. Olsen, R.P. Mitchell, A. Davis, S.J. Rowland, A.W.G. John, D. McGonigle, A.E. Russell, Lost at sea: Where does all the plastic go? Science 304 (2004) 838.
[6] K. Waldschläger, S. Lechthaler, G. Stauch, H. Schüttrumpf, The way of microplastic through the environment – Application of the source-pathway-receptor model (review), Sci. Total Environ. 713 (2020) 136584, https://doi.org/10.1016/j.scitotenv.2020.136584.
[7] Q. Sun, S.-Y. Ren, H.-G. Ni, Incidence of microplastics in personal care products: An appreciable part of plastic pollution, Sci. Total Environ. 742 (2020) 140218, https://doi.org/10.1016/j.scitotenv.2020.140218.
[8] A.R.A. Lima, M.F. Costa, M. Barletta, Distribution patterns of microplastics within the plankton of a tropical estuary, Environ. Res. 132 (2014) 146–155, https://doi.org/10.1016/j.envres.2014.03.031.
[9] C. Accinelli, H.K. Abbas, W.T. Shier, A. Vicari, N.S. Little, M.R. Aloise, S. Giacomini, Degradation of microplastic seed film-coating fragments in soil, Chemosphere 226 (2019) 645–650, https://doi.org/10.1016/j.chemosphere.2019.03.161.
[10] A.A. Horton, A. Walton, D.J. Spurgeon, E. Lahive, C. Svendsen, Microplastics in freshwater and terrestrial environments: Evaluating the current understanding to identify the knowledge gaps and future research priorities, Sci. Total Environ. 586 (2017) 127–141.
[11] F. De Falco, E. Di Pace, M. Cocca, M. Avella, The contribution of washing processes of synthetic clothes to microplastic pollution, Sci. Rep. 9 (1) (2019), https://doi.org/10.1038/s41598-019-43023-x.
[12] J.K.H. Wong, K.K. Lee, K.H.D. Tang, P.-S. Yap, Microplastics in the freshwater and terrestrial environments: Prevalence, fates, impacts and sustainable solutions, Sci. Total Environ. 719 (2020) 137512, https://doi.org/10.1016/j.scitotenv.2020.137512.
[13] R. Dris, J. Gasperi, V. Rocher, M. Saad, N. Renault, B. Tassin, Microplastic contamination in an urban area: a case study in Greater Paris, Environ. Chem. 12 (5) (2015) 592, https://doi.org/10.1071/EN14167.
[14] R. Di Mauro, M.J. Kupchik, M.C. Benfield, Abundant plankton-sized microplastic particles in shelf waters of the northern Gulf of Mexico, Environ. Pollut. 230 (2017) 798–809, https://doi.org/10.1016/j.envpol.2017.07.030.
[15] J. Wang, Y. Li, L. Lu, M. Zheng, X. Zhang, H. Tian, W. Wang, S. Ru, Polystyrene microplastics cause tissue damages, sex-specific reproductive disruption and transgenerational effects in marine medaka (Oryzias melastigma), Environ. Pollut. 254 (2019) 113024, https://doi.org/10.1016/j.envpol.2019.113024.
[16] G. Li, W. Zhu, L. Zhu, X. Chai, Effect of pyrolytic temperature on the adsorptive removal of p-benzoquinone, tetracycline, and polyvinyl alcohol by the biochars from sugarcane bagasse, Korean J. Chem. Eng. 33 (7) (2016) 2215–2221, https://doi.org/10.1007/s11814-016-0067-9.
[17] X. Liu, J. Xu, Y. Zhao, H. Shi, C.-H. Huang, Hydrophobic sorption behaviors of 17β-Estradiol on environmental microplastics, Chemosphere 226 (2019) 726–735, https://doi.org/10.1016/j.chemosphere.2019.03.162.
[18] C. Li, R. Busquets, L.C. Campos, Assessment of microplastics in freshwater systems: A review, Sci. Total Environ. 707 (2020) 135578, https://doi.org/10.1016/j.scitotenv.2019.135578.
[19] J.L. Lavers, S. Oppel, A.L. Bond, Factors influencing the detection of beach plastic debris, Marine Environmental Research 119 (2016) 245–251, https://doi.org/10.1016/j.marenvres.2016.06.009.
[20] J.-L. Xu, K.V. Thomas, Z. Luo, A.A. Gowen, FTIR and Raman imaging for microplastics analysis: State of the art, challenges and prospects, TrAC, Trends Anal. Chem. 119 (2019) 115629, https://doi.org/10.1016/j.trac.2019.115629.
[21] J. shan, J. Zhao, L. Liu, Y. Zhang, X. Wang, F. Wu, A novel way to rapidly monitor microplastics in soil by hyperspectral imaging technology and chemometrics, Environ. Pollut. 238 (2018) 121–129, https://doi.org/10.1016/j.envpol.2018.03.026.
[22] F. Corradini, H. Bartholomeus, E. Huerta Lwanga, H. Gertsen, V. Geissen, Predicting soil microplastic concentration using vis-NIR spectroscopy, Sci. Total Environ. 650 (2019) 922–932, https://doi.org/10.1016/j.scitotenv.2018.09.101.
[23] J. Masura, J. Baker, G. Foster, A. Courtney, Laboratory Methods for the Analysis of Microplastics in the Marine Environment: recommendations for quantifying synthetic particles in waters and sediments, NOAA Tech. Memo. NOS-OR&R-4 (2015) 39, https://marinedebris.noaa.gov/sites/default/files/publications-files/noaa_microplastics_methods_manual.pdf.
[24] R.K.H. Galvão, M.C.U. Araujo, G.E. José, M.J.C. Pontes, E.C. Silva, T.C.B. Saldanha, A method for calibration and validation subset partitioning, Talanta 67 (4) (2005) 736–740, https://doi.org/10.1016/j.talanta.2005.03.025.
[25] M. Andersson, A comparison of nine PLS1 algorithms, J. Chemometrics 23 (10) (2009) 518–529, https://doi.org/10.1002/cem.1248.
[26] A. de Araújo Gomes, R.K.H. Galvão, M.C.U. de Araújo, G. Véras, E.C. da Silva, The successive projections algorithm for interval selection in PLS, Microchem. J. 110 (2013) 202–208, https://doi.org/10.1016/j.microc.2013.03.015.
[27] A.C. Olivieri, H.C. Goicoechea, F.A. Iñón, MVC1: an integrated MatLab toolbox for first-order multivariate calibration, Chemomet. Intell. Lab. Syst. 73 (2) (2004) 189–197, https://doi.org/10.1016/j.chemolab.2004.03.004.
[28] Y.K. Song, S.H. Hong, M. Jang, G.M. Han, M. Rani, J. Lee, W.J. Shim, A comparison of microscopic and spectroscopic identification methods for analysis of microplastics in environmental samples, Mar. Pollut. Bull. 93 (1-2) (2015) 202–209, https://doi.org/10.1016/j.marpolbul.2015.01.015.